Supporting Information

One-pot synthesis of high-flux *b*-oriented MFI zeolite membranes for Xe recovery

Xuerui Wang,[†, *] Pelin Karakiliç,[‡] Xinlei Liu,[†] Meixia Shan,[†] Arian Nijmeijer,[‡] Louis Winnubst,[‡] Jorge Gascon,[†, §, *] and Freek Kapteijn[†, *]

[†] Chemical Engineering Department, Delft University of Technology, Van der Maasweg 9, 2629 HZ Delft, The Netherlands

[‡] Department Inorganic Membranes, MESA+ Institute for Nanotechnology, University of Twente, P.O. Box 217, 7500 AE Enschede, The Netherlands

[§] KAUST Catalysis Center, Advanced Catalytic Materials, King Abdullah University of Science and Technology, Thuwal 23955, Saudi

Corresponding Author

* Xuerui Wang, x.wang-12@tudelft.nl
* Jorge Gascon, jorge.gascon@kaust.edu.sa
* Freek Kapteijn, f.kapteijn@tudelft.nl

This supporting information file includes: Supporting Figure S1 to S13, Supporting Table S1 to S5.

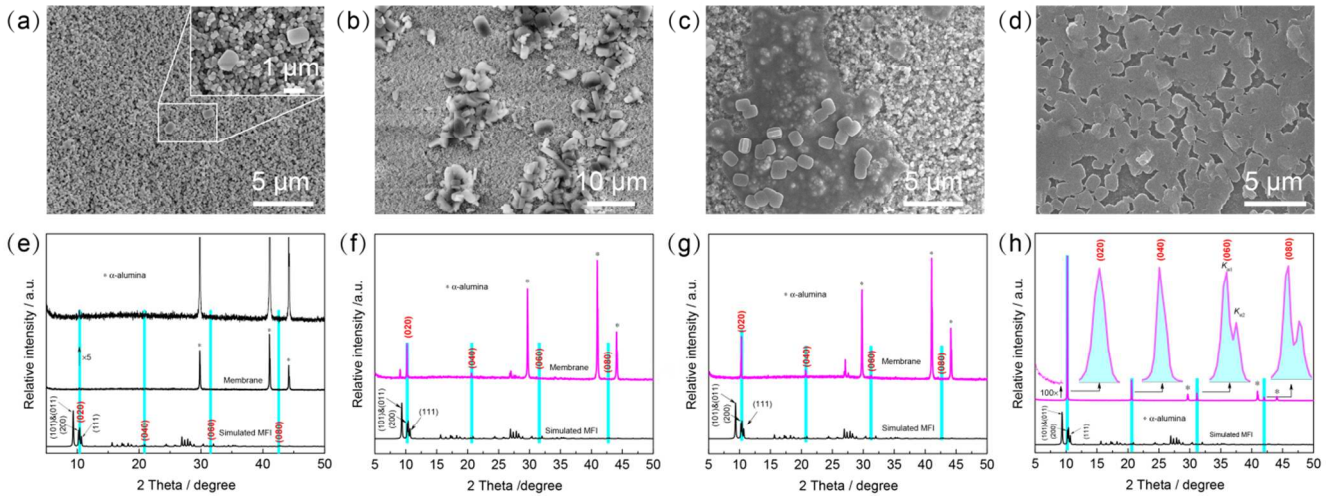

Figure S1. SEM images and PXRD patterns of MFI membranes prepared by *in-situ* crystallization on different substrates. (a, e) 80-nm alumina, 3 h (M1); (b, f) 80-nm alumina, 8 h (M2); (c, g) 80-nm alumina dip-coated by 2% colloid silica sol, 2 h (M3); (d, h) Home-made silica-coated alumina, 2 h (M5). Synthesis condition: 1 TEOS: 0.2 TPAOH: 110 H_2O at 150 °C.

After *in-situ* crystallization of 3 h, only scattered MFI crystals could be observed from the alumina surface (**Figure S1**a). No reflections could be detected from PXRD because of the small amount of zeolite crystals (**Figure S1**e). However, the crystal preferred to random stacking as hillocks rather than a film when the synthesis time was prolonged to 8 h (**Figure S1**b). It is interesting to mention that several MFI crystals well aligned together if the alumina substrate was dip-coated by 2% colloid silica sol prior to the *in-situ* crystallization (**Figure S1**c, f). We speculate the Si source in the substrate facilitates the nucleation and growth of MFI crystals. Our hypothesis is further approved by the microporous silica-coated alumina substrate, which can supply the Si source for MFI nucleation and growth (**Figure S1**d). The monolayered MFI crystals are totally *b*-oriented (**Figure S1**h).

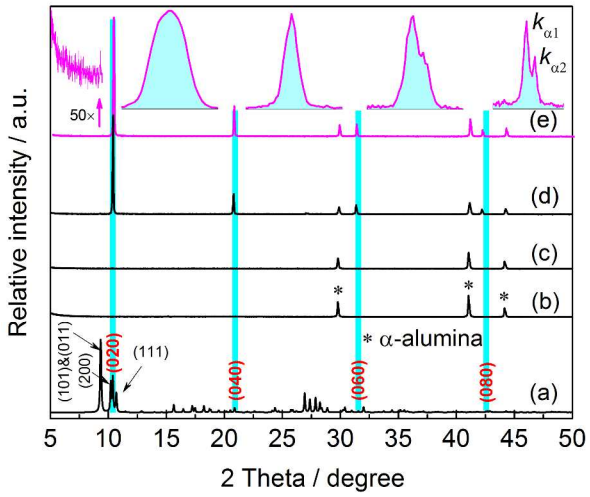

Figure S2. PXRD patterns of home-made silica-coated alumina support and MFI zeolite membranes (M4-M6) prepared by *in-situ* crystallization. (a) Simulated PXRD of MFI zeolite; (b) Silica-coated alumina support; (c-e) *b*-oriented MFI zeolite membrane synthesized for 1 h, 2 h, and 3 h, respectively. Synthesis condition: 1 TEOS: 0.2 TPAOH: 110 H_2O at 150 °C.

The diffraction of MFI crystals could be detected after 2 h of *in-situ* crystallization (**Figure S2**d-e). It should be noted that only the diffraction peaks from (020), (040), (060) and (080) planes are detected, confirming that the crystals are indeed *b*-oriented. The diffraction peak from (101) and (011) planes is hardly observed even after 50 × magnification (**Figure S2**e).

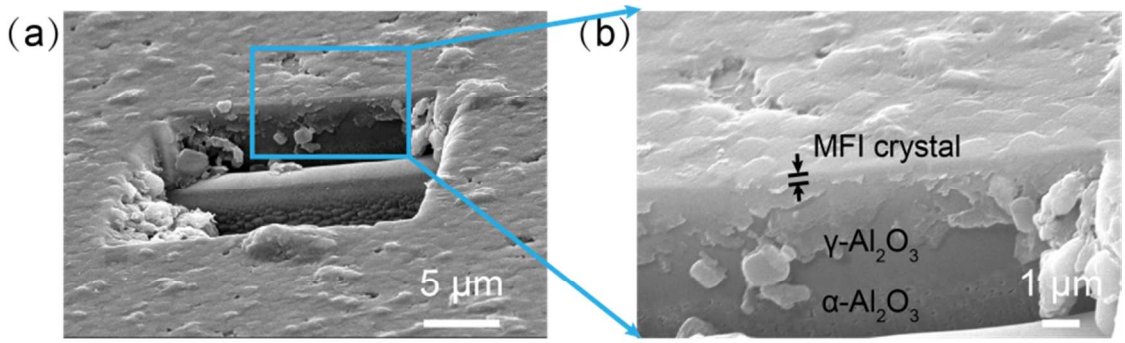

Figure S3. Low- (a) and high-magnified (b) FIB-SEM images of *b*-oriented MFI monolayer (M6) prepared by *in-situ* crystallization on home-made silica-coated alumina support at 150 °C for 3 h.

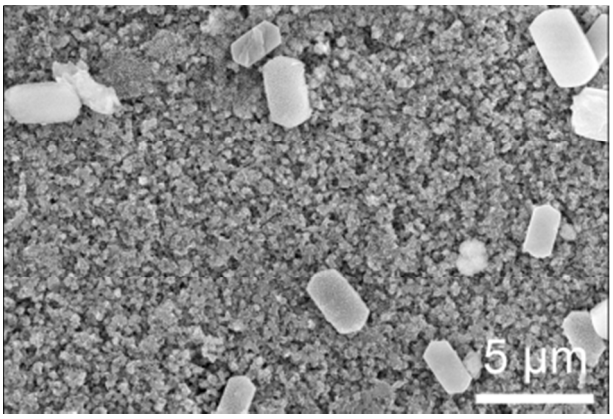

Figure S4. SEM image of MFI crystals (M10) prepared by *in-situ* crystallization on home-made silica-coated alumina support from Si-free synthesis solution. Synthesis condition: 0 TEOS: 0.2 TPAOH: 110 H_2O at 150 °C for 8 h.

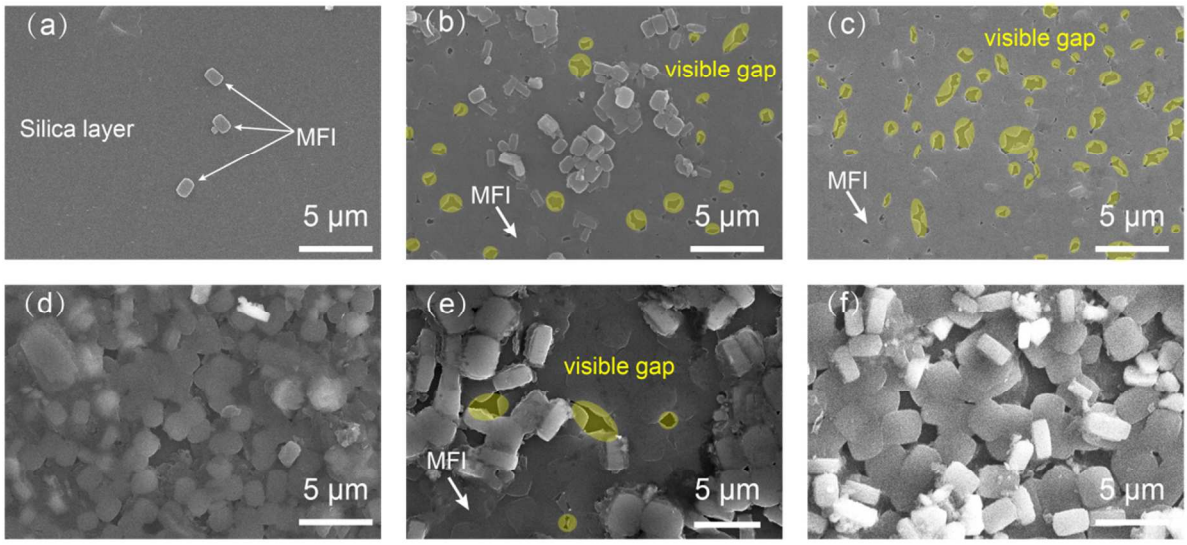

Figure S5. SEM images of *b*-oriented MFI membranes (M4-M9) prepared by *in-situ* crystallization at different periods. (a) 1 h; (b) 2 h; (c) 3 h; (d) 4 h; (e) 5 h; (f) 6 h. Synthesis condition: 1 TEOS: 0.2 TPAOH: 110 H_2O at 150 °C.

Only scattered MFI crystals could be observed from the home-made silica-coated support after *in-situ* crystallization of 1 h at 150 °C (**Figure S5**a), consistent with PXRD results (**Figure S2**). A semi-continuous layer was formed after 2 h and visible gaps (highlighted in yellow color) could be observed within the membrane layer (**Figure S5**b-e). It is difficult to eliminate the visible gaps in the *b*-oriented MFI crystal layer by increasing the period for *in-situ* crystallization (**Figure S5**f).

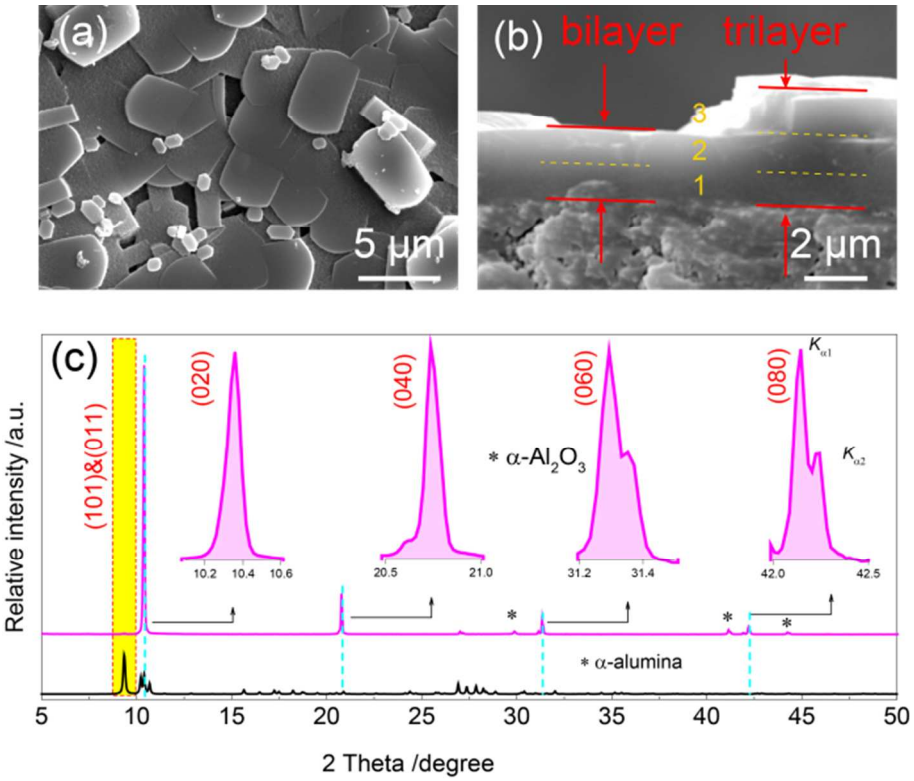

Figure S6. SEM images (a-b) and PXRD pattern (c) of *b*-oriented MFI zeolite membrane M17. The membrane was prepared by *in-situ* crystallization in 1 TEOS: 0.2 TPAOH: 110 H_2O at 150 °C for 10 h with 0.1 wt.% TBPO.

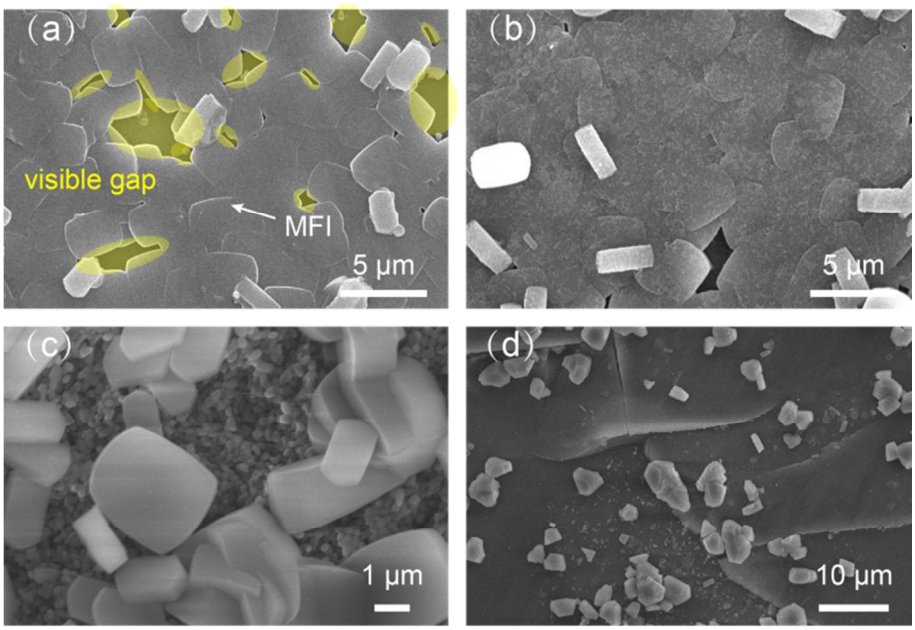

Figure S7. SEM images of MFI zeolite membranes (M12-M15) *in-situ* crystallized on home-made silica-coated alumina support with different concentration of TBPO. (a) 0.2 wt.%; (b) 0.3 wt.%; (c) 0.4 wt.%; (d) 0.5 wt.%; Synthesis condition: 1 TEOS: 0.2 TPAOH: 110 H_2O at 150 °C for 6 h.

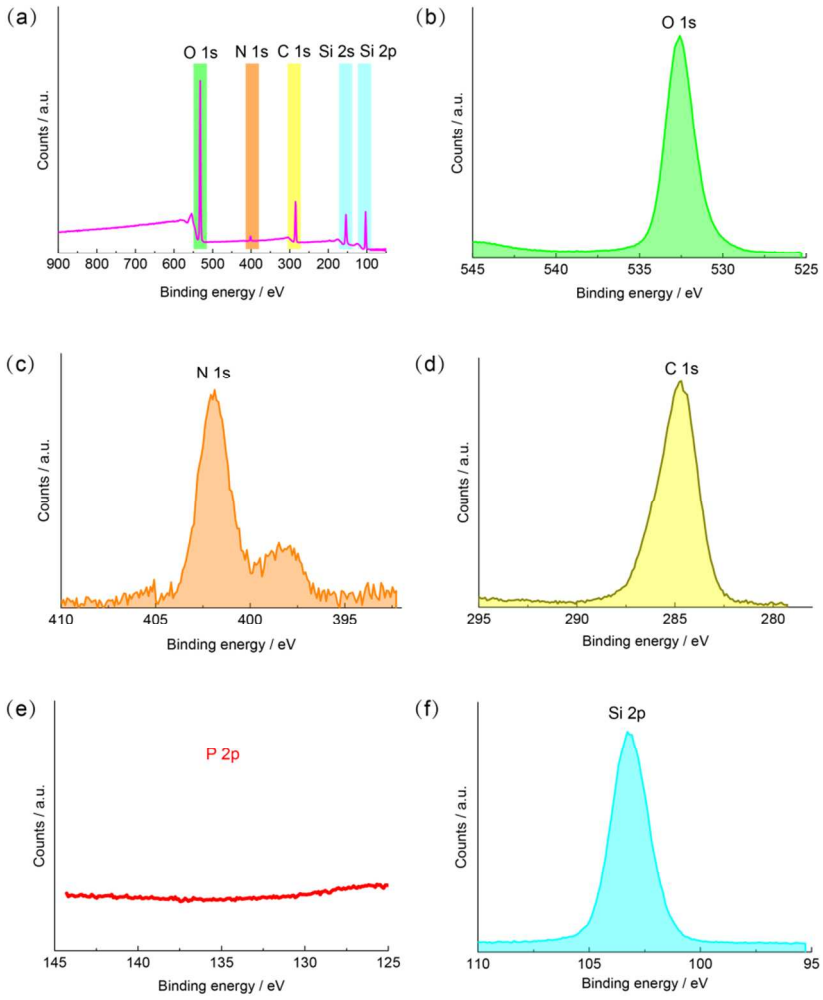

Figure S8. (a) Full scan and (b-f) O1s, N1s, C1s, P2p and Si2p XPS spectra of *b*-oriented MFI zeolite membrane M11 on silica-coated alumina support before calcination.

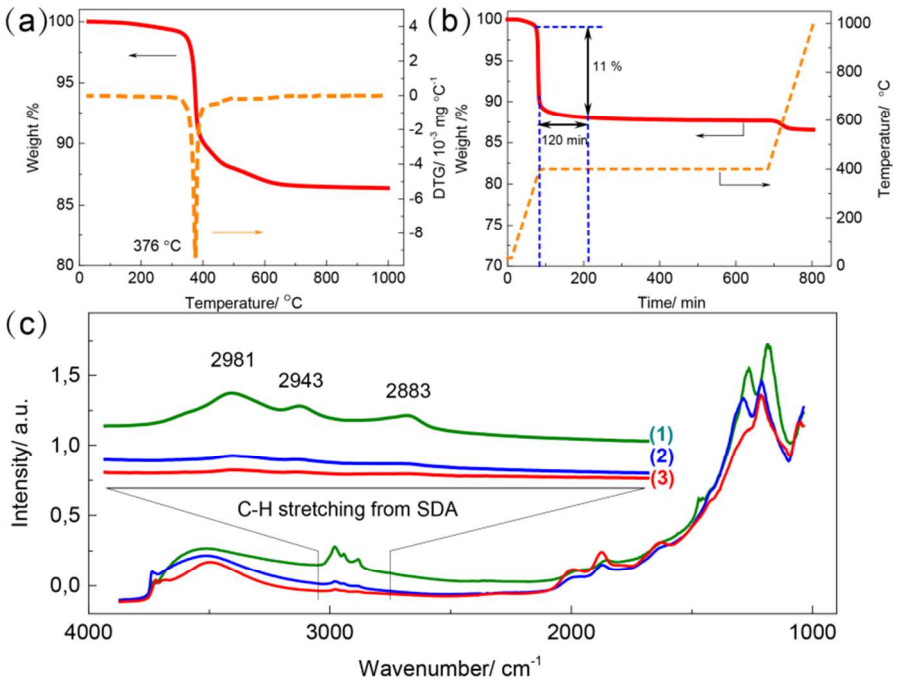

Figure S9. Template removal from MFI zeolite powder and MFI zeolite membrane. (a) TGA curves of SDA-containing MFI zeolite powder under air atmosphere from room temperature to 1000 °C with a heating rate of 10 °C/min; (b) TGA curves of SDA-containing MFI zeolite powder under air atmosphere; (c) FTIR spectra of *b*-oriented MFI zeolite membrane (M11) before calcination (1), calcined at 400 °C for 1 h (2), and calcined at 400 °C for 2 h (3).

As demonstrated by the TGA (**Figure S9**a), the organic template trapped in MFI zeolite channels began to decompose from 350 °C. The decomposition mainly occurred below the temperature of 400 °C (**Figure S9**b). Further, we can calculate a mass loss of approximate 11 % after calcination at 400 °C for 2 h. As reported by Nagy *et al.*, TPA^+ cations are always occluded intact in the pores and that each channel intersection contained one TPA^+ species, equally 3.68 TPA^+ per unit cell.[1] Thus, the mass loss in **Figure S9**b matches well with theory. The effective removal of the organic template was further confirmed by FTIR spectra as shown in **Figure S9**c. The bands centered at 2981, 2943 and 2883 cm^{-1} are assigned to the C-H stretching vibrations from methyl ($-CH_3$) and methylene ($-CH_2-$) groups associated with the presence of the SDA.[2] These bands are not present anymore in the spectrum of the samples after calcination at 400 °C for 2 h.

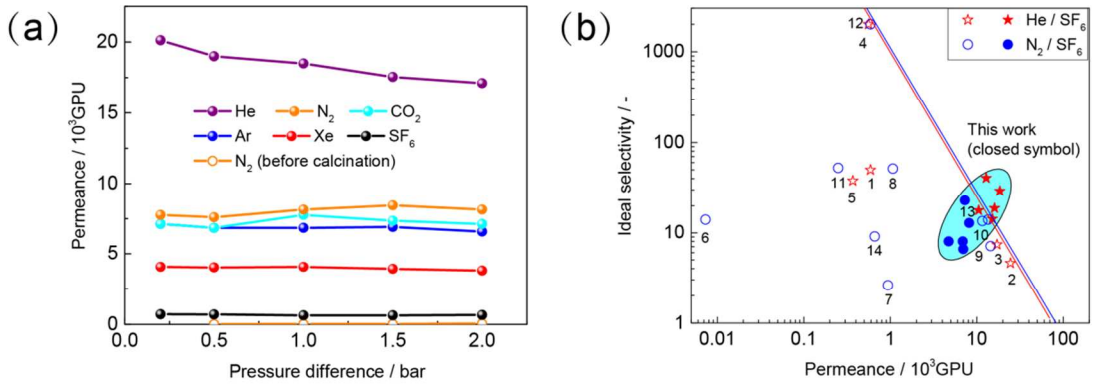

Figure S10. Single gas permeation performance of *b*-oriented MFI zeolite membranes. (a) Pressure-dependent single gas permeance at room temperature (M11); (b) Separation performance comparison of five MFI zeolite membranes in this work for He/SF_6 and N_2/SF_6. The data points from literatures plotted in (b) are listed in **Table S4**.

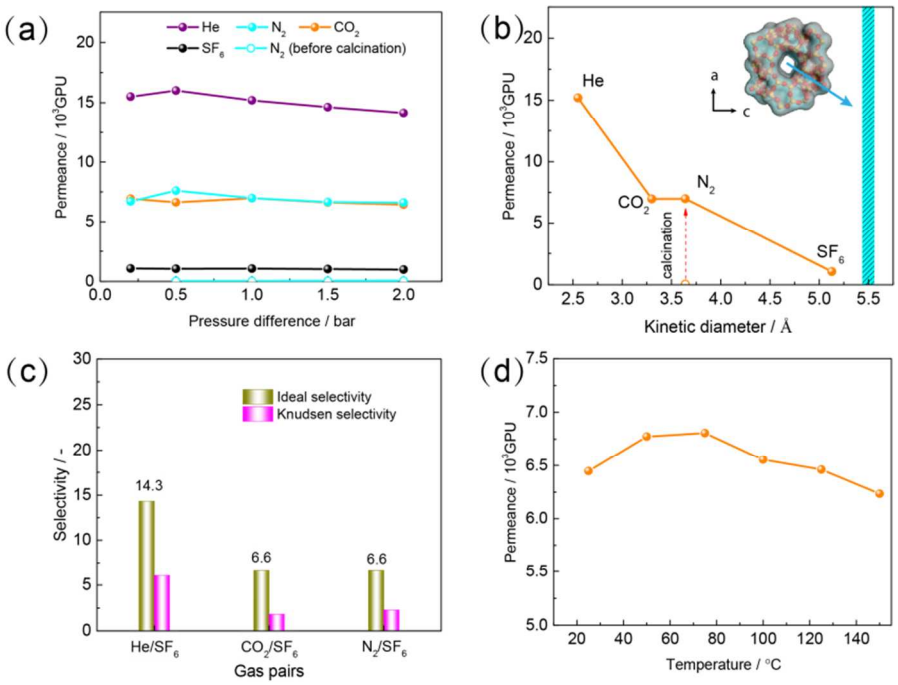

Figure S11. Single gas permeation performance of *b*-oriented MFI zeolite membrane M18. (a) Pressure-dependent single gas permeance at room temperature; (b) Cut-off of single gas permeance at room temperature and an absolute pressure of 2 bar; (c) Ideal selectivity of light gas molecules to SF_6; (d) Temperature-dependent CO_2 permeance at an absolute pressure of 3 bar.

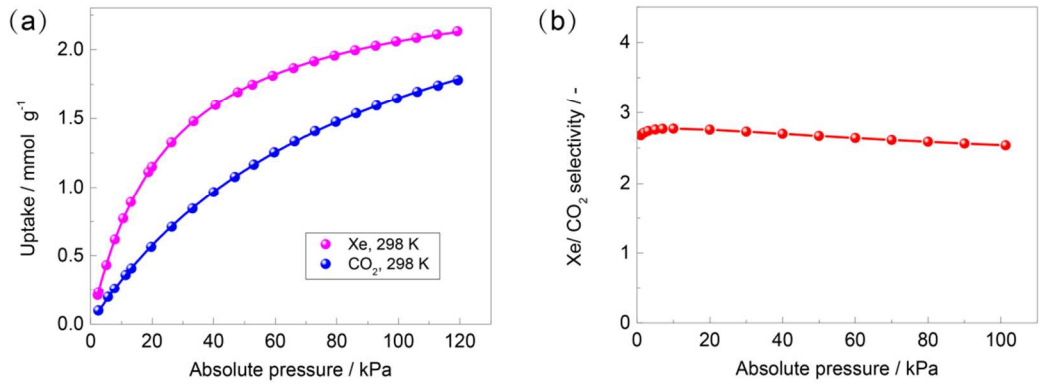

Figure S12. (a) Xe and CO_2 isotherms on MFI zeolite at 298 K; Solid lines represent the fits of the single-site Langmuir-Freundlich equation. (b) Xe/CO_2 adsorption selectivity calculated based on IAST theory.

The adsorption selectivity for an equimolar CO_2/Xe mixture was calculated with the ideal adsorbed solution theory (IAST).[3] This theory allows prediction of mixture loading based on single component adsorption isotherms and is generally assumed applicable for zeolite systems. The input parameters were obtained by fitting the adsorption isotherm data with a single-site Langmuir-Freundlich model and shown in Table S6.

$$q = \frac{q_{sat} \cdot K \cdot p^m}{1 + K \cdot p^m} \quad (1)$$

where q is the total quantity of adsorbed CO_2 or Xe, mmol g^{-1}; p is the partial pressure, kPa; q_{sat} is termed the saturation loading, mmol g^{-1}; K is Langmuir adsorption constant, kPa^{-1}; m is the Langmuir-Freundlich exponent.

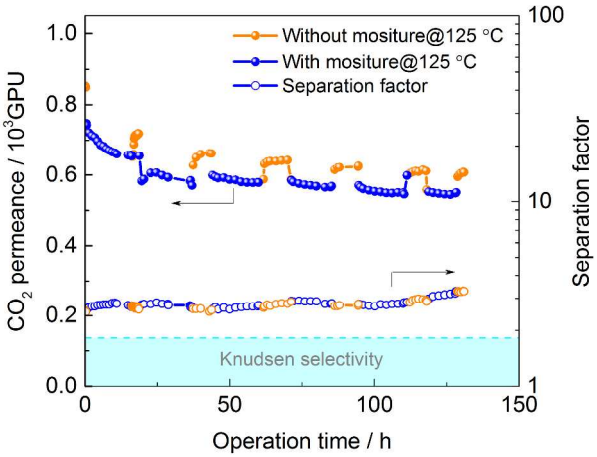

Figure S13. Long-term stability of *b*-oriented MFI zeolite membrane for the separation of a 50/50 CO_2/SF_6 mixture saturated with 2.3 kPa water vapour at 125 °C.

Considering the high price of Xe, we demonstrated the long-term hydrothermal stability of *b*-oriented MFI zeolite membrane for the separation of CO_2/SF_6 mixtures instead of CO_2/Xe. The feed gas was saturated with 2.3 kPa water vapour before feeding into the membrane at 125 °C. The CO_2 permeance gradually decreased once water vapour was introduced. The membrane performance stabilized after 30 h. The membrane permeance can be easily recovered by drying at 125 °C. This indicates the decreased permeance cannot be attributed to structural degradation. We attribute this to the competitive adsorption of H_2O, CO_2, and SF_6.

Table S1.Summary of preparation parameters of MFI zeolite membranes in this work.

Sample	Support	TBPO / wt.%	Time / h
M1	Alumina	0	3
M2	Alumina	0	8
M3	Alumina[b]	0	2
M4	SiO_2/ α-alumina[c]	0	1
M5	SiO_2/ α-alumina[c]	0	2
M6	SiO_2/ α-alumina[c]	0	3
M7	SiO_2/ α-alumina[c]	0	4
M8	SiO_2/ α-alumina[c]	0	5
M9	SiO_2/ α-alumina[c]	0	6
M10[a]	SiO_2/ α-alumina[c]	0	6
M11	SiO_2/ α-alumina[d]	0.1	6
M12	SiO_2/ α-alumina[c]	0.2	6
M13	SiO_2/ α-alumina[c]	0.3	6
M14	SiO_2/ α-alumina[c]	0.4	6
M15	SiO_2/ α-alumina[c]	0.5	6
M16	α-alumina	0.1	8
M17	SiO_2/ α-alumina[d]	0.1	10
M18	SiO_2/ α-alumina[d]	0.1	10

[a], synthesized from Si-free solution with a composition of 0.2 TPAOH: 110 H_2O; [b], dip-coated by 2% colloid silica sol; [c], home-made; [d], purchased from Fraunhofer IKTS Hermsdorf.

Table S2. Crystallographic preferred orientation (CPO) of MFI zeolite membranes in this work.

Sample[a]	Support	TBPO / wt.%	Time / h	$CPO_{(020)/(501)}$	Orientation
M5	SiO_2/ α-alumina	0	2	99.1 %	*b*
M6	SiO_2/ α-alumina	0	3	99.8 %	*b*
M9	SiO_2/ α-alumina	0	6	99.7 %	*b*
M11	SiO_2/ α-alumina	0.1	6	99.6 %	*b*
M16	α-alumina	0.1	8	68.8 %	*random*
M18	SiO_2/ α-alumina	0.1	10	98.0 %	*b*

[a], synthesis condition: 1 TEOS: 0.2 TPAOH: 110 H_2O at 150 °C.

Table S3. Single gas permeance of *b*-oriented MFI zeolite membranes in this work.

Sample[a]	Feed	Pressure / bar[b]	Temperature / °C	P_{He} / GPU	S_{He/SF_6}
M11	He or SF_6	2	25	18500	29.2
M17[c]	He or SF_6	2	25	14900	18.8
M18[c]	He or SF_6	2	25	15200	14.3

[a], synthesis condition: 1 TEOS: 0.2 TPAOH: 110 H_2O at 150 °C; [b], absolute pressure; [c], prepared by the same procedure.

Table S4. Single gas permeance of MFI zeolite membranes from literature.[4-12]

Sample	Thickness/ μm	Orientation	Feed	Pressure / bar[a]	Temperature / °C	P_i / GPU [b]	S_{i/SF_6} [c]	Reference
1	3	*random*	He or SF_6	2	25	590	50	4
2	0.55	*a*	He or SF_6	2	25	24520	4.6	5
3	0.55	*a*	He or SF_6	2	25	17150	7.4	5
4	2	*random*	He or SF_6	5	20	560	2000	6
5	2	*random*	He or SF_6	2	25	370	38	4
6	N.A.	*N.A.*	N_2 or SF_6	N.A.	N.A.	7.3	14	8
7	1	*b*	N_2 or SF_6	1	220	940	2.6	9
8	1	*h0h / c*	N_2 or SF_6	2	25	1075	51.5	10
9	0.55	*a*	N_2 or SF_6	2	25	14500	7.1	5
10	0.55	*a*	N_2 or SF_6	2	25	11590	13.5	5
11	N.A.	*N.A.*	N_2 or SF_6	2	25	250	52.5	11
12	2	*random*	N_2 or SF_6	5	25	590	2000	6
13	2	*random*	N_2 or SF_6	1.4	25	13558	14.0	7
14	1~2	*random*	N_2 or SF_6	2	25	660	9.1	12

[a], absolute pressure; [b], He or N_2 permeance; [c], Ideal selectivity of He or N_2 to SF_6.

Table S5. CO_2/Xe separation performance of various membrane materials.[13-16]

Number	Membrane	Feed	Pressure / bar[a]	Temperature / °C	P_{CO_2} / GPU	$S_{CO_2/Xe}$	Reference
1	Carbon molecular sieve	4.55/ 66.15/4.75/ 24.55 CO_2/ Xe/ N_2/ O_2	2	27	23.2	160[b]	[13]
2	SAPO-34	CO_2 or Xe	1	22	295	500[c]	[14]
3	PIM-1	CO_2 or Xe	1	30	49.5	41.8[c]	[15]
4	PIM-7	CO_2 or Xe	1	30	38.9	41.3[c]	[15]
5	PDMS	CO_2 or Xe	1.7	30	14.2	1.4[c]	[16]
6	*b*-oriented MFI zeolite (M11)	50/ 50 CO_2/ Xe	1.5	75	1213	5.3	This work
7	*b*-oriented MFI zeolite (M11)	50/ 50 CO_2/ Xe	1.5	175	1196	5.6	This work
8	*b*-oriented MFI zeolite (M19)	50/ 50 CO_2/ Xe	1.2	75	2154	3.6	This work

[a], absolute pressure; [b], separation factor; [c], ideal selectivity.

Table S6. Adsorption isotherm parameter values estimated for CO_2 and Xe.

Gas	Temperature/ K	q_{sat} / mmol g^{-1}	K / kPa^{-1}	m
Xe	298	2.5529	0.03936	1.0129
CO_2	298	3.1558	0.01159	0.9876

REFERENCES

(1) Nagy, J. B.; Gabelica, Z.; Derouane, E. G., Position and Configuration of the Guest Organic Molecules within the Framework of the ZSM-5 and ZSM-11 Zeolites. *Zeolites* **1983,** *3*, 43-49.

(2) Tiriolo, R.; Rangnekar, N.; Zhang, H.; Shete, M.; Bai, P.; Nelson, J.; Karapetrova, E.; Macosko, C. W.; Siepmann, J. I.; Lamanna, E.; Lavano, A.; Tsapatsis, M., Sub-Micrometer Zeolite Films on Gold-Coated Silicon Wafers with Single-Crystal-Like Dielectric Constant and Elastic Modulus. *Adv. Funct. Mater.* **2017,** *27*, 1700864.

(3) Myers, A. L.; Prausnitz, J. M., Thermodynamics of Mixed-Gas Adsorption. *AIChE J.* **1965,** *11*, 121-127.

(4) Kanezashi, M.; O'Brien, J.; Lin, Y. S., Template-Free Synthesis of MFI-Type Zeolite Membranes: Permeation Characteristics and Thermal Stability Improvement of Membrane Structure. *J. Membr. Sci.* **2006,** *286*, 213-222.

(5) Rezai, S. A. S.; Lindmark, J.; Andersson, C.; Jareman, F.; Möller, K.; Hedlund, J., Water/Hydrogen/Hexane Multicomponent Selectivity of Thin MFI Membranes with Different Si/Al Ratios. *Microporous Mesoporous Mater.* **2008,** *108*, 136-142.

(6) Lassinantti, M.; Jareman, F.; Hedlund, J.; Creaser, D.; Sterte, J., Preparation and Evaluation of Thin ZSM-5 Membranes Synthesized in the Absence of Organic Template Molecules. *Catal. Today* **2001,** *67*, 109-119.

(7) Algieri, C.; Bernardo, P.; Golemme, G.; Barbieri, G.; Drioli, E., Permeation Properties of a Thin Silicalite-1 (MFI) Membrane. *J. Membr. Sci.* **2003,** *222*, 181-190.

(8) Smetana, J. F.; Falconer, J. L.; Noble, R. D., Separation of Methyl Ethyl Ketone from Water by Pervaporation Using a Silicalite Membrane. *J. Membr. Sci.* **1996,** *114*, 127-130.

(9) Lai, Z.; Tsapatsis, M., Gas and Organic Vapor Permeation through *b*-Oriented MFI Membranes. *Ind. Eng. Chem. Res.* **2004,** *43*, 3000-3007.

(10) Xiao, W.; Yang, J.; Lu, J.; Wang, J., Preparation and Characterization of Silicalite-1 Membrane by Counter-Diffusion Secondary Growth. *J. Membr. Sci.* **2009,** *345*, 183-190.

(11) Sebastián, V.; Kumakiri, I.; Bredesen, R.; Menéndez, M., Zeolite Membrane for CO_2 Removal: Operating at High Pressure. *J. Membr. Sci.* **2007,** *292*, 92-97.

(12) Çulfaz, P. Z.; Çulfaz, A.; Kalıpçılar, H., Preparation of MFI Type Zeolite Membranes in a Flow System with Circulation of the Synthesis Solution. *Microporous Mesoporous Mater.* **2006,** *92*, 134-144.

(13) Lagorsse, S.; Magalhães, F. D.; Mendes, A., Xenon Recycling in an Anaesthetic Closed-System Using Carbon Molecular Sieve Membranes. *J. Membr. Sci.* **2007,** *301*, 29-38.

(14) Wu, T.; Lucero, J.; Zong, Z.; Elsaidi, S. K.; Thallapally, P. K.; Carreon, M. A., Microporous Crystalline Membranes for Kr/Xe Separation: Comparison between AlPO-18, SAPO-34, and ZIF-8. *ACS Appl. Nano Mater.* **2018,** *1*, 463-470.

(15) Budd, P. M.; Msayib, K. J.; Tattershall, C. E.; Ghanem, B. S.; Reynolds, K. J.; McKeown, N. B.; Fritsch, D., Gas Separation Membranes from Polymers of Intrinsic Microporosity. *J. Membr. Sci.* **2005,** *251*, 263-269.

(16) Malankowska, M.; Martins, C. F.; Rho, H. S.; Neves, L. A.; Tiggelaar, R. M.; Crespo, J. G.; Pina, M. P.; Mallada, R.; Gardeniers, H.; Coelhoso, I. M., Microfluidic Devices as Gas – Ionic Liquid Membrane Contactors for CO_2 Removal from Anaesthesia Gases. *J. Membr. Sci.* **2018,** *545*, 107-115.